metals

MDPI

Article

The Role of Grain Boundaries in the Corrosion Process of Fe Surface: Insights from ReaxFF Molecular Dynamic Simulations

Zigen Xiao [1], Yun Huang [2], Zhixiao Liu [1,*], Wangyu Hu [1], Qingtian Wang [3] and Chaowei Hu [3,*]

[1] College of Materials Science and Engineering, Hunan University, Changsha 410082, China; xiaozigeng@hnu.edu.cn (Z.X.); wyuhu@hnu.edu.cn (W.H.)
[2] School of Physics and Electronics, Hunan University, Changsha 410082, China; huangyun19@hnu.edu.cn
[3] Key Laboratory of Nuclear Reactor System Design Technology, Nuclear Power Institute of China, Chengdu 610041, China; wqtian@126.com
* Correspondence: zxliu@hnu.edu.cn (Z.L.); npichd10@npic.ac.cn(C.H.)

Abstract: Intergranular corrosion is the most common corrosion phenomenon in Fe-based alloys. To better understand the mechanism of intergranular corrosion, the influence of grain boundaries on Fe-H_2O interfacial corrosion was studied using molecular dynamics simulation based on a new Fe-H_2O reaction force field potential. It is found that the corrosion rate at the polycrystalline grain boundary is significantly faster than that of twin crystals and single crystals. By the analysis of stress, it can be found that the stress at the polycrystalline grain boundary and the sigma5 twin grain boundary decreases sharply during the corrosion process. We believe that the extreme stress released at the grain boundary will promote the dissolution of Fe atoms. The formation of vacancies on the Fe matrix surface will accelerate the diffusion of oxygen atoms. This leads to the occurrence of intergranular corrosion.

Keywords: ReaxFF; corrosion; Fe-H_2O interface; grain boundary

Citation: Xiao, Z.; Huang, Y.; Liu, Z.; Hu, W.; Wang, Q.; Hu, C. The Role of Grain Boundaries in the Corrosion Process of Fe Surface: Insights from ReaxFF Molecular Dynamic Simulations. *Metals* **2022**, *12*, 876. https://doi.org/10.3390/met12050876

Academic Editor: Amir Mostafaei

Received: 6 April 2022
Accepted: 17 May 2022
Published: 21 May 2022

1. Introduction

Fe-based alloys are widely used as structural materials [1] because of their excellent tensile strength and high toughness [2]. However, the corrosion of metal in the working environment will reduce the mechanical properties of metal and shorten its service life. In the corrosion process, the metal is electrochemically oxidized into ions or some compounds [3]. In particular, the presence of grain boundaries can cause intergranular corrosion. The dissolution rate of Fe atoms in the grain boundary region is much greater than the dissolution rate of crystal grains, leading to local corrosion [4]. Intergranular corrosion refers to the boundaries of crystallites of the material being more susceptible to corrosion than their insides, which is mainly caused by the difference in chemical composition between the surface and the interior of the grains and the existence of internal stress.

The surface structure of the Fe-based alloys is complex with defects such as grain boundaries, corners, edges, boundaries, interference layers, etc. [5,6]. Corrosion usually occurs at the defect first, and the corrosion at the defect is more severe than inside the crystal. It can be observed in the experiments that the corrosion is more severe at the grain boundary compared with the inside of the crystal [7]. You et al. found that the corrosion in pure Fe is initiated by pits that quickly become blocked and that it propagates around the pits giving rise to the formation of porous layers [8]. The grain refinement obtained by rolling improved the corrosion resistance of iron in sulfuric acid solution, borate buffer solution, and borate buffer solution with chloride ion [9]. Bennett et al. studied the influence of orientation angle and grain boundary structure on grain boundary corrosion of austenitic and ferritic stainless steels. They pointed out that the grain boundary corrosion mechanism is not only the dissolution of the chromium-depleted alloy but also other mechanisms, but the specific mechanism is not distinct [10]. According to Lapeire's study, grain orientation

can also affect corrosion behavior, and the orientation of adjacent grains plays a dominant role in the dissolution rate [11]. The reduction of the electronic work function at the grain boundary indicates the electrons at the grain boundary are more active, which makes the grain boundary vulnerable to electrochemical attack [12]. Emily et al. believed that the corrosion at the grain boundary is caused by the combined effect of sensitization and crevice corrosion. The precipitation of chromium and the grain boundary has set the local corrosion sensitivity [13].

Up to now, the density functional theory calculations (DFT) and reaction force field (ReaxFF) molecular dynamics (MD) simulations have been usually used to study Fe and Fe-water surface corrosion mechanisms. Hu et al. studied the effects of four typical surface adsorbates [14]. Their works suggested that the strong interaction between oxygen and surface will weaken the bonds' strength between substrate atoms, which will lead to structure deformation and charge redistribution in the substrate. In addition, Bucun et al. studied the effects of oxygen precovering and water adsorption on the surface of Fe substrates [15]. The time and space scales of the above simulations are seriously limited, which can only describe the trend and cannot carry out the complete dynamic evolution of the corrosion process. The ReaxFF-MD provides an alternative method to simulate the interface reaction and can explain the effect of defects (such as grain boundaries) on corrosion from stress changes and energy changes [16,17]. Verners et al. [18] studied nickel-based alloys' stress corrosion cracking behavior. The existence of stress will hinder the twin dislocation failure and activate the new slip to reduce the strength of nickel. DorMohammadi et al. used ReaxFF-MD to study the initial stage of Fe corrosion in pure water under different applied electric fields and temperatures and then studied the passivation mechanism of Fe substrate and the depassivation process of chloride [19–21]. The study of Klu et al. showed that the existence of polycrystalline grain boundaries could significantly increase the diffusion coefficient of carbon, and the release of stress can reduce the diffusion barrier of carbon [22].

In summary, defects in pure iron will preferentially corrode during the corrosion process. Whether the grain boundary as a typical defect will affect the surface corrosion process of pure iron. The computational methods involving simulations of dynamic processes are an important tool for understanding the mechanism of dynamic processes in reactive systems, such as corrosion. The present article, using a reactive force field (ReaxFF) molecular dynamics (MD) simulation, highlights the effect of grain boundaries on the evolution of the corrosion process in a reactive pure Fe-H_2O system.

2. Computational Details

In this study, three kinds of Fe models—single crystal, sigma3 or sigma5 twins, and polycrystalline—were used to study the influence of grain boundary on the corrosion process of pure Fe-H_2O surface systems. The sigma3 twin boundary is composed of the (111) plane, and the sigma5 twins plane is composed of the (02-1) plane. The structure at the twin grain boundary is stable and the interfacial energy is low. However, the polycrystalline grain boundary structure is unstable, the lattice distortion is large, and there are many defects. The stress in this paper is the shear stress of the Fe substrate on the Y-axis. It is obtained by counting the stress sum of Fe atoms at the grain boundary in the Y direction and dividing it by the corresponding total atomic volume. The volume of polycrystalline grains is 35 nm^3. The schematic diagram of the models is shown in Figure 1. The Fe substrate comprises twelve atom layers in the polycrystalline simulation system, including 9215 Fe atoms and existing many defects such as grain boundaries and stacking fault. The water-side part includes the water layers of 40 Å thickness with the density of 0.99 g/cm^3 (about 4669 water molecules at 300 K and 1 atm).

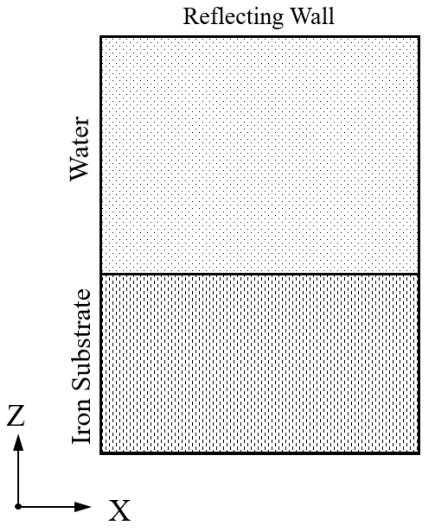

Figure 1. Schematic diagram of the simulation model for the Fe-water surface system.

All the simulations were based on the open-source Large-scale Atomic/Molecular Massively Parallel Simulator (LAMMPS) code [23] and the atomic interactions were described using the ReaxFF for pure Fe-H_2O systems. The original ReaxFF was developed by van Duin et al. [24]. The ReaxFF-MD can simulate the chemical reaction process that includes chemical bonds breaking and forming between atoms; therefore, it is suitable for studying interfacial corrosion. Recently, our group developed a new Fe-H_2O ReaxFF potential function [25], which can accurately describe the nature of the defects in Fe substrate and the Fe-water interactions. The interaction between vacancy and hydrogen/oxygen is emphasized to describe the precipitation of hydrogen/oxygen near the vacancy. The energy contributions to the Fe-H_2O ReaxFF potential are summarized by the following [25]:

$$E_{system} = E_{bond} + E_{over} + E_{under} + E_{val} + E_{lp} + E_{Coul} + E_{H-bond} + E_{vdW} \quad (1)$$

which includes terms related to bond, angle, over coordination, undercoordination, lone pair, van der Waals, Coulomb, and H-bond energies. The details of the ReaxFF potential have been shown in our recent paper. The essential part of ReaxFF is that the charge equilibration (QEq) method can be used to obtain the charge distribution [26,27]. The charge values were determined at each simulation time step and depended on the system's geometry. This feature made it possible to describe charge transfer in chemical reactions using ReaxFF. Subsequently, this study did not consider an absolute stress value analysis, instead focusing on relations between reactivity and stress states.

The periodic boundary conditions were applied in the *X*- and *Y*-directions in all simulated boxes, and the *Z*-direction uses aperiodic boundary conditions. A reflective wall is added at the upper Z boundary to prevent atoms from passing through the boundary. The Fe substrate and water molecules are relaxed with a Nose/Hoover isothermal–isobaric (NPT) [28] to reach equilibrium. Nose–Hoover thermostat [29,30] is used to maintain the prescribed system temperature during corrosion for the canonical (NVT) ensemble. The MD simulation time step is 0.2 fs. The corrosion process of the pure Fe-H_2O system was observed by external electric field [31] acceleration at 300 K and NVT ensemble, which is located at 0~3 Å on the surface of the Fe substrate. We chose the most suitable external electric field to be 325 MV/cm by observing the corrosion phenomenon. All subsequent simulations are performed under this electric field strength. The relationship between

individual atomic charges and the corresponding electrostatic energy $E(\mathbf{q})$ with time is shown in Equation (2):

$$E(\mathbf{q}) = \sum_{i=1}^{N} \left[\chi_i q_i + \eta_i q_i^2 + Tap(r_{ij}) k_c \frac{q_i q_j}{\left(r_{ij}^3 + \gamma_{ij}^{-3} \right)} \right] \quad (2)$$

where $\mathbf{q}$ represents a vector of length N containing the charges, q_i is the charge of ion i, N is the total number of ions, k_c is the dielectric constant, χ_i and η_i are represent the electronegativity and the hardness of ion i, $Tap(r)$ is a seventh-order taper function, and γ_{ij} refers to the shielding parameter between the two atoms I and j.

We reproduced their works to verify the correctness of the ReaxFF potential according to the article of DorMohammadi et al. [19]. The simulation models mainly consist of body-centered cubic (bcc) Fe and water molecules. The corrosion processes of low-index surfaces (100), (110), and (111) were accelerated by applying an external electrical field. The corrosion phenomenon is consistent compared with the works of DorMohammadi et al. The difference is that the diffusion of H atoms into the substrate can be clearly observed during the corrosion process. Therefore, we believe that the ReaxFF potential parameters can simulate Fe-water interfacial corrosion accelerated by an external electric field at room temperature. The relevant verification process is in the supporting materials.

3. Results

The Corrosion Process at the Grain Boundary

In order to study the corrosion process of a perfect crystal, we simulate the pure Fe-H_2O interfacial corrosion of Fe (110) single crystal for that the (110) surface is the most stable close-packed one. The corrosion processes of the single crystal are shown in Figure 2. It can be found that water molecules are adsorbed on the surface of the Fe substrate at 0.14 ps (Figure 2a); then the hydrogen-oxygen bond of the water molecule begins to stretch (Figure 2b); and finally, the water molecules decomposed completely into OH^- and free H^+ ions (Figure 2c). The chemical reaction during the corrosion process is shown below:

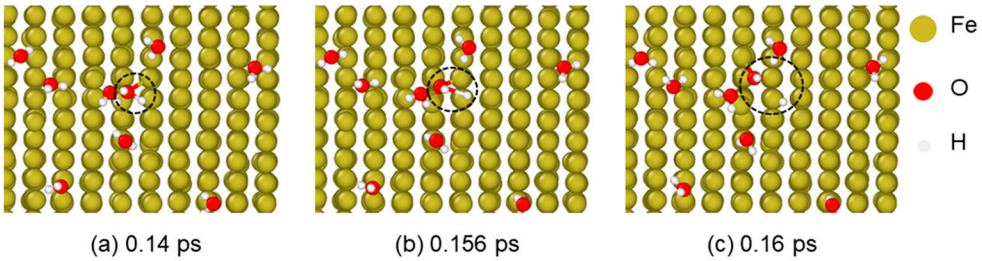

Figure 2. (**a**) The adsorption of water molecules on the Fe substrate; (**b**) the elongation of the O-H bond in the adsorbed water molecules; and (**c**) the breaking of the O-H bond and the formation of OH^-.

Step 1: The water molecules adsorbed on the surface of the Fe substate dissociate to form OH^- and H^+:

$$H_2O \rightarrow OH^- + H^+$$

OH^- is adsorbed on the surface of the substrate to generate Fe(OH):

$$Fe + OH^- \rightarrow FeOH + e^-$$

The charge of the Fe atoms on the surface rises to 0.4 e, and the charge of the O atoms drops to −0.69 e.

Step 2: The Fe(OH) on the surface dissolves into the water:

$$Fe + FeOH + OH^- \rightarrow FeOH + FeOH^+ + 2e^-$$

The charge of the Fe atoms on the surface rises to 0.57 e
Step 3: Fe is oxidized to form Fe^{2+}:

$$FeOH^{+} + H^{+} \rightarrow Fe^{2+} + H_2O$$

Step 4: The adsorbed OH^{-} also dissociate into O and H ions, forming additional H^3O^{+} and iron oxides.

During the process of the adsorption of H_2O on the surface of Fe substrate to form $Fe(OH)_2$, the surface Fe atoms are oxidized, and the average charge increases to 0.7 e. The O atoms adsorbed on the surface are reduced and the average charge drops to −0.775 e, H ions also penetrate into the Fe substrate with an average charge of −0.25 e. Finally, the adsorbed OH^{-} also dissociate into O and H ions, forming additional H_3O^{+} and iron oxides.

In Fe single crystal, O ions penetration uniformly into the Fe substrate to form oxides (Figure 3a). The Fe (110) surface with a sigma3 twins is also studied, as shown in Figure 3b. It can be found that the corrosion process of the sample with sigma3 twins is similar to that of single crystals. After water molecules decompose on the Fe surface, Fe atoms will dissolve into the water solution, O ions will penetrate into the Fe substrate to form oxides, and H ions will diffuse into the Fe substrate. The existence of the twin grain boundary does not affect the corrosion rate of the Fe substrate. This situation is because the sigma3 grain boundaries are relatively stable and not easy to corrode.

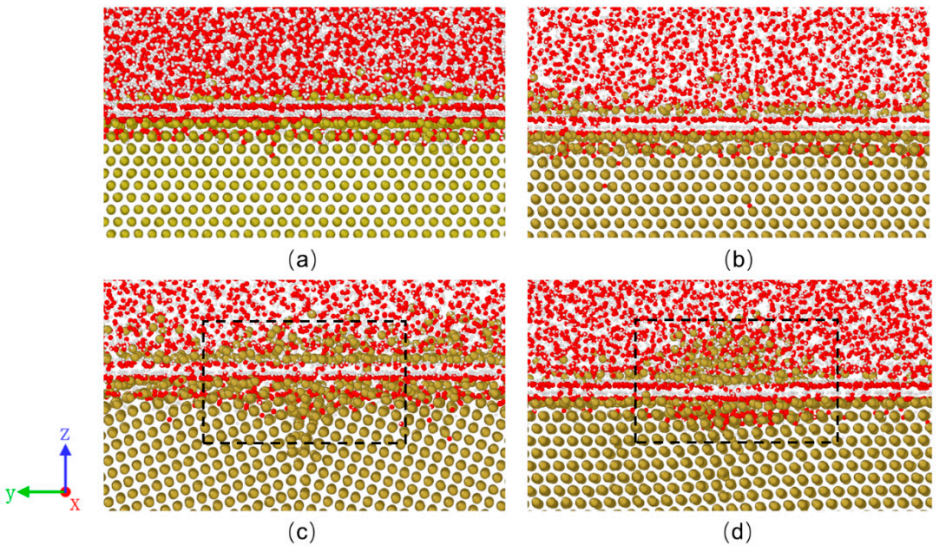

Figure 3. The snapshots at different corrosion stages for the different pure Fe-H_2O models in 300 K: (**a**) Fe single crystal (110); (**b**) Fe sigma3 (110) [111] twins; (**c**) Fe sigma5 (02-1) [012] twins; (**d**) polycrystals. The yellow, red, and white spheres represent Fe, oxygen, and hydrogen atoms.

However, the corrosion of sigma5 twins is different from that of sigma3 twins. The most stable (210) surface is used to test the effect of different grain boundaries on corrosion. As shown in Figure 3c, the penetration of O ions at the grain boundary is faster, and the corrosion depth at the grain boundary is more than four atomic layers. This phenomenon is related to the structure and stability of the grain boundary. As the angle of the grain boundary increases, the corrosion at the grain boundary will be easier.

To verify the above speculation, we simulate the corrosion of the polycrystalline grain boundary. According to Figure 3d, polycrystalline consists of three grains, and irregular grain boundaries are obtained by rotating the grain in the middle. The corrosion phenomenon of polycrystal is similar to sigma5 twins, but the phenomenon of grain boundary corrosion is more prominent. Many Fe atoms on the grain boundary are dissolved and O ions penetrate rapidly into the grain boundaries to form oxides. The number of dissolved Fe atoms in polycrystals is far greater than that of sigma5 twins, and the corrosion

rate of grain boundaries is speedy. This may be related to the reduction of Fe work function (ionization energy) during H_2O adsorption obtained by the multielectron intercalation theory [17] and may also be related to stress.

It is found that O ions penetrate faster at the polycrystalline and sigma5 twin grain boundaries, and local corrosion occurs at the grain boundaries, as shown in Figure 4. In the polycrystalline model, O ions first penetrate into the grain boundaries and then along the grain boundaries to the surroundings to form oxides. In the twinned system, a small number of O ions are distributed on the sigma5 twin grain boundary. However, it is impossible to judge whether it penetrates along the grain boundaries, and the O ions in the sigma3 twins exhibit uniform penetration. During the corrosion process, the stress changes at the grain boundaries, as shown in Figure 5. The stress at the polycrystalline grain boundary decreases in a wide range during the corrosion process, and the stress at the sigma5 twin is only reduced at the grain boundary, but the stress at the sigma3 twin remains unchanged. The variation range of stress is consistent with the penetration range of O ions.

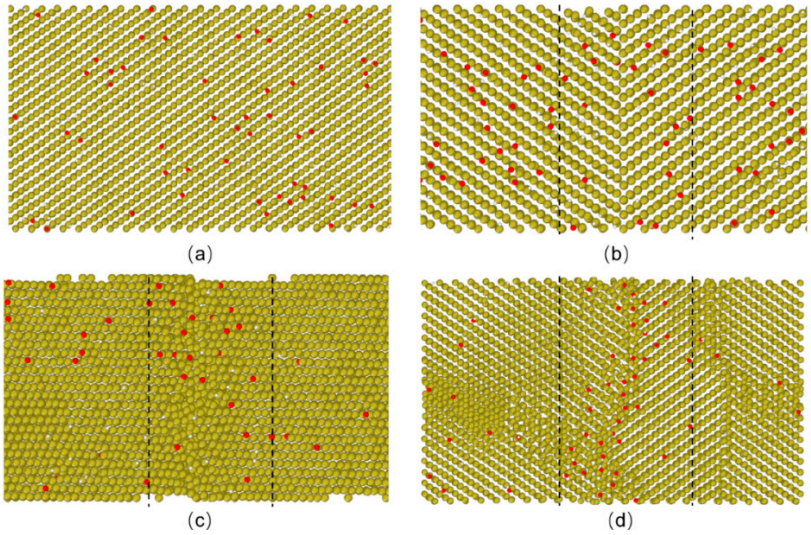

Figure 4. Distribution of oxygen atoms in Fe substrate during corrosion. (**a**) Fe single crystal (110); (**b**) Fe sigma3 (110) [111] twins; (**c**) Fe sigma5 (02-1) [012] twins; (**d**) polycrystals.

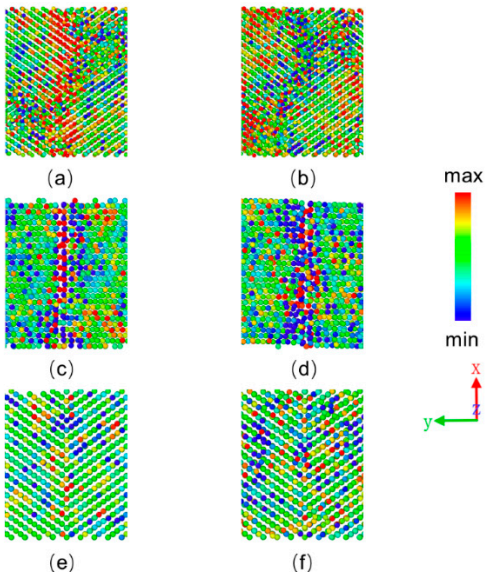

Figure 5. The stress change of the Fe substrate during the corrosion process. (**a**,**b**) are the polycrystalline; (**c**,**d**) are the sigma5 twins; (**e**,**f**) are the sigma3 twins.

4. Discussion

4.1. The Principle of Grain Boundary Corrosion

Figure 6 shows the variation of shear stress in the Y-direction of the iron substrate; the vertical axis is the difference between the initial stress and the instantaneous stress. During the corrosion process, the stress at the polycrystalline grain boundary was reduced by 2.0 GPa within 200 ps, the stress at the sigma5 twin boundary was reduced by 1.25 GPa, and the sigma3 twin boundary was only reduced by 0.75 GPa, but the stress of the single crystal remained unchanged. The changing trend of stress corresponds to the corrosion phenomenon of the model. Therefore, we believe that the enormous stress relief in the high-stress region at the grain boundary will deform the grain boundary structure and cause the atoms at the grain boundary to dissolve, leaving many vacancies on the surface. The existence of vacancies accelerates the diffusion of O ions, thereby promoting the corrosion of grain boundaries.

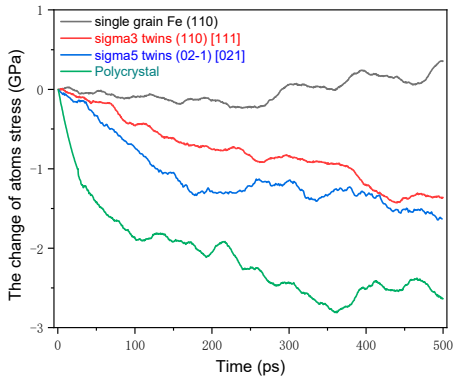

Figure 6. Changes in shear stress of polycrystalline and twin models over simulation time.

The effects of different grain boundaries on the corrosion process were compared by counting the number of dissolved Fe atoms near the grain boundaries and the number of O ions diffused into the Fe substrate. According to Figure 7a, the number of dissolved Fe atoms in polycrystalline and sigma5 twins is the largest due to the early stress release. Within 50 ps, about 250 Fe atoms are dissolved from polycrystalline, and about 100 Fe atoms are dissolved from sigma5 twins. The number of dissolved iron atoms in sigma3 twins and single crystals is roughly the same. Figure 7b shows the number of O ions penetrating into the vicinity of the grain boundaries of the iron substrate. It can be seen that a large number of iron atoms at the grain boundaries of the polycrystalline model are dissolved, and most vacancies are formed on the surface, which causes O ions to penetrate into the substrate quickly. Therefore, the polycrystalline model has the most oxygen atoms penetrating into the substrate. Approximately 100 O ions in sigma5 twins penetrate into the substrate. The number of oxygen atoms in sigma3 twins is 20 more than that in single crystals, but the number of dissolved Fe atoms is the same.

Corrosion at grain boundaries is always accompanied by the massive dissolution of Fe atoms at grain boundaries. Therefore, we simulated the effect of the concentration of vacancies in the Fe substrate on the penetration of O ions in corrosion. Randomly add vacancies in the Fe substrate, and the vacancy concentration is 0%, 5%, and 10%. The result is shown in Figure 8. The concentration of vacancies affects the penetration and depth of O ions penetrate. When the vacancy concentration is 5%, the penetration depth of O ions only increases by 0.25 Å, but when the vacancy concentration rises to 10%, the penetration depth of O ions increases by 1.5 Å. We can conclude that the concentration of vacancies in the Fe substrate reaches a certain level, and O ions can quickly penetrate into the bulk. In intergranular corrosion, the excessive initial stress of the grain boundary causes a large number of Fe atoms at the grain boundary to dissolve to form vacancies, which makes it easier for O ions to penetrate into the substrate to form oxides in accelerated local corrosion.

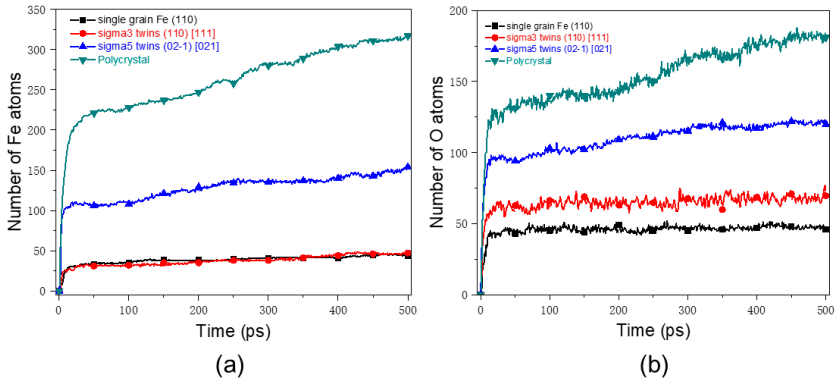

Figure 7. (**a**) The number of Fe atoms dissolved into H_2O over time. (**b**) The number of O atoms diffused into the substrate over time.

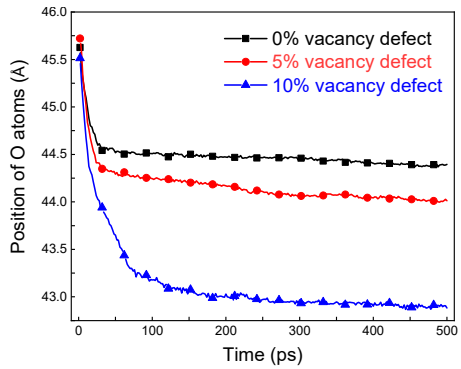

Figure 8. The effect of vacancy concentration on the diffusion of oxygen atoms. The curve represents the average position of oxygen atom diffusion. Simulate by randomly adding vacancies to the Fe substrate proportionally.

4.2. Characterization of Corrosion at the Grain Boundary

The dynamic evolution of the chemical composition of the Fe/water interface system is shown in Figure 9a. In the early 5 ps of corrosion, due to the adsorption and dissociation of many water molecules, a large number of byproducts such as H_3O^+, H_2, OH^-, and H atoms are generated, which means that the early corrosion rate is high. After 10ps, the system enters the slow-corrosion state. After the dissociation of water molecules, O ions diffuse into the Fe substrate, and H ions enter the solution to form H_3O^+. Therefore, as the corrosion progresses, the amount of H_3O^+ gradually increases. Figure 9b shows the changes in the number of water molecules over the simulation time. To avoid interference, we only count the changes of water molecules above the grain boundaries. The changing trend of water molecules in all models is the same. The significant reduction of water molecules in the first 50 ps means a faster corrosion rate. After the initial passivation, the number of water molecules slowly decreases. As the angle of the grain boundary increases, the number of water molecules decreases. It also shows that the existence of grain boundaries will affect the adsorption and dissociation of water molecules and the subsequent penetration of oxygen atoms.

The atomic charge distribution at the end of the pure Fe-H_2O system simulation is depicted in Figure 10. The charge of the Fe atoms at the bottom of the metal substrate has fluctuated around 0 e. The charges of O and H atoms in the solution fluctuate slightly around −0.775 e and 0.320 e, respectively. These atomic charges are consistent with the previous simulation articles [19]. Charge exchange mainly occurs in the electric double layer, where the Fe atom loses electrons, and the charge of the surface Fe atoms rises to nearly 0.7 e. In addition, the charge of oxygen atoms diffused into the Fe substrate decreases to 0.3 e. When hydrogen atoms enter the Fe substrate as interstitial atoms or combine with Fe atoms in the solution, the hydrogen atoms possess a specific negative charge of about

0.2 e. In contrast, the hydrogen atoms in the OH^- ions still carry a positive charge. The related research reveals that the H atoms spread into the Fe substrate possess a negative charge [32,33]. Therefore, during the corrosion process, there is a process of redistribution of electric charge on the pure Fe-H_2O system.

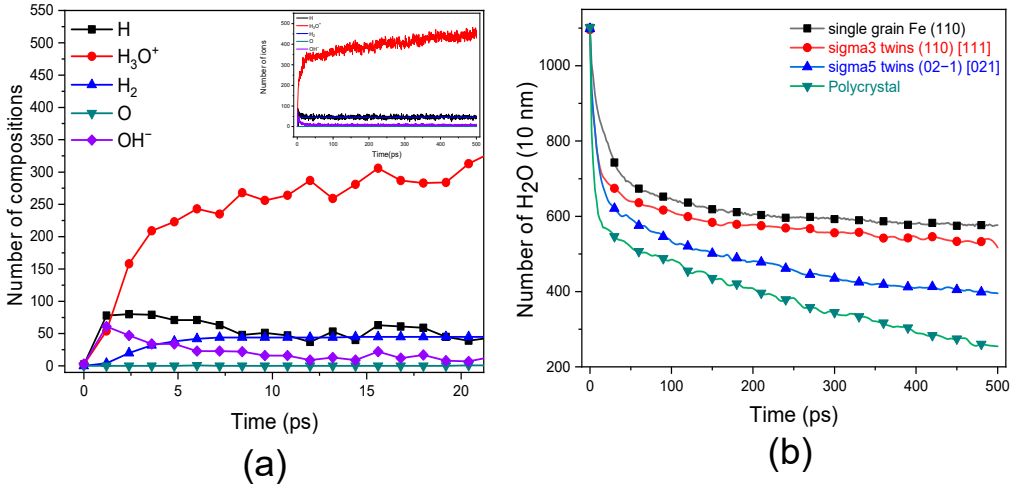

Figure 9. (**a**) The change of ions numbers of polycrystalline during the simulation time and (**b**) the evolution of water molecules in the simulation time.

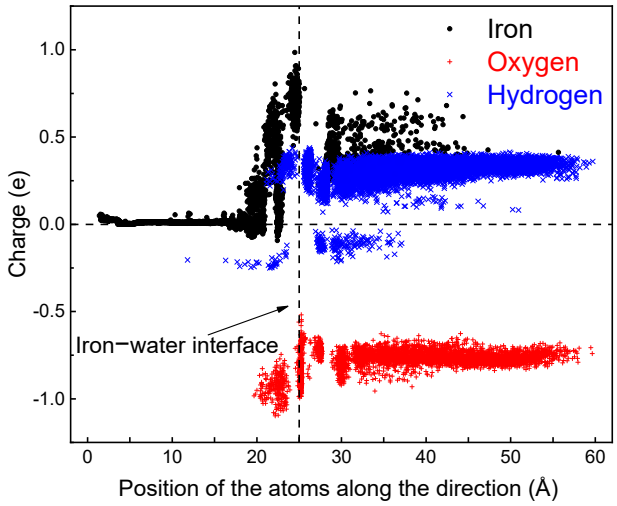

Figure 10. Charge distributions of the polycrystal pure Fe-H_2O system at 500 ps.

The radial distribution functions (RDFs) can study the different Fe oxide phases in simulation can be studied by the radial distribution functions (RDFs). Generally, the partial radial distribution function (RDF), g (r), defined as the probability of an atom at a distance from the origin, which is used to characterize the bonding and the structure of the formed oxide film [34,35]. Figure 11 shows the RDFs for the O-H bond and the Fe-O bond at the end of the simulation. The RDFs were calculated every 0.4 ps and took an average of 450 to 500 ps. It has two prominent peaks for the Fe-O bond length. The first peaks at 1.78 Å correspond to the interaction of Fe ions and OH- ions, but this peak spans from 1.5 Å to 2.5 Å covering the peaks of FeO, Fe_2O_3, and Fe_3O_4. These results show that the oxide film formed on the Fe surface mainly consists of Fe hydroxides and oxides in the corrosion process. The transformation trend is the transformation of Fe hydroxide to Fe oxide.

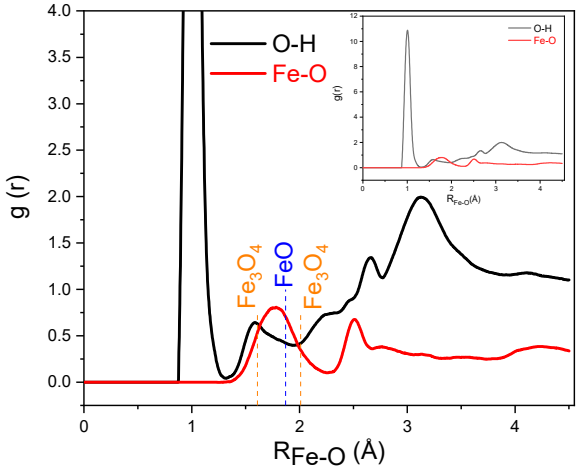

Figure 11. Partial radial distribution functions for the oxide film of polycrystal model at 500 ps.

5. Conclusions

In this paper, the reactive molecular dynamics simulation method studied the effect of different grain boundaries on the corrosion interface process of pure Fe-H_2O. Our study shows that the stress release in the high-stress region of the grain boundary during the corrosion process promotes the rapid penetration of O ions into the grain boundary to form oxides, resulting in the occurrence of intergranular corrosion in pure iron. The effect of grain boundaries on intergranular corrosion is revealed from the point of view of simulation, which provides a theoretical explanation for the occurrence of intergranular corrosion in Fe-H_2O corrosion in a realistic environment.

Author Contributions: Conceptualization, Z.L. and C.H.; methodology, Z.L. and C.H.; validation, Z.X. and Y.H.; formal analysis, Z.X.; investigation, Z.X.; data curation, Z.X.; writing—original draft preparation, Z.X.; writing—review and editing, Z.X., Y.H., W.H., C.H. and Q.W.; funding acquisition, Q.W. All authors have read and agreed to the published version of the manuscript.

Funding: This work was supported by the research project for Hua-long Pressurized Reactor (HPR1000) in China National Nuclear Corporation.

Data Availability Statement: Data sharing not applicable.

Conflicts of Interest: The authors declare no conflict of interest.

References

1. Sherif, E.-S.M.; Almajid, A.A.; Khalil, K.A.; Junaedi, H.; Latief, F. Electrochemical studies on the corrosion behavior of API X65 pipeline steel in chloride solutions. *Int. J. Electrochem. Sci.* **2013**, *8*, 9360–9370.
2. Čapek, J.; Stehlíková, K.; Michalcová, A.; Msallamová, Š.; Vojtěch, D. Microstructure, mechanical and corrosion properties of biodegradable powder metallurgical Fe-2 wt% X (X= Pd, Ag and C) alloys. *Mater. Chem. Phys.* **2016**, *181*, 501–511. [CrossRef]
3. Kutz, M. *Handbook of Environmental Degradation of Materials*; William Andrew: Norwich, NY, USA, 2018.
4. Galvele, J.; de De Micheli, S. Mechanism of intergranular corrosion of Al-Cu alloys. *Corros. Sci.* **1970**, *10*, 795–807. [CrossRef]
5. Gwathmey, A. Effect of Crystal Orientation on Corrosion. In *The Corrosion Handbook*; Uhlig, H.H., Ed.; John Wiley & Sons, Inc.: Hoboken, NJ, USA, 1948; Volume 33, pp. 157–162.
6. Zou, Y.; Wang, J.; Zheng, Y. Electrochemical techniques for determining corrosion rate of rusted steel in seawater. *Corros. Sci.* **2011**, *53*, 208–216. [CrossRef]
7. Schultze, J.; Davepon, B.; Karman, F.; Rosenkranz, C.; Schreiber, A.; Voigt, O. Corrosion and passivation in nanoscopic and microscopic dimensions: The influence of grains and grain boundaries. *Corros. Eng. Sci. Technol.* **2004**, *39*, 45–52. [CrossRef]
8. You, D.; Pebere, N.; Dabosi, F. An investigation of the corrosion of pure iron by electrochemical techniques and in situ observations. *Corros. Sci.* **1993**, *34*, 5–15. [CrossRef]
9. Jinlong, L.; Hongyun, L. The effects of cold rolling temperature on corrosion resistance of pure iron. *Appl. Surf. Sci.* **2014**, *317*, 125–130. [CrossRef]
10. Bennett, B.W.; Pickering, H.W. Effect of grain boundary structure on sensitization and corrosion of stainless steel. *Metall. Trans. A* **1991**, *18*, 1117–1124. [CrossRef]

11. Lapeire, L.; Lombardia, E.M.; Verbeken, K.; De Graeve, I.; Kestens, L.; Terryn, H. Effect of neighboring grains on the microscopic corrosion behavior of a grain in polycrystalline copper. *Corros. Sci.* **2013**, *67*, 179–183. [CrossRef]
12. Li, D. Electron work function at grain boundary and the corrosion behavior of nanocrystalline metallic materials. *MRS Online Proc. Libr.* **2005**, *887*, 8870503. [CrossRef]
13. Hoffman, E.E.; Lin, A.; Liao, Y.; Marks, L.D. Grain boundary assisted crevice corrosion in CoCrMo alloys. *Corrosion* **2016**, *72*, 1445–1461. [CrossRef]
14. Hu, J.; Wang, C.; He, S.; Zhu, J.; Wei, L.; Zheng, S. A DFT-Based Model on the Adsorption Behavior of H_2O, H^+, Cl^-, and OH^- on Clean and Cr-Doped Fe (110) Planes. *Coatings* **2018**, *8*, 51. [CrossRef]
15. Nunomura, N.; Sunada, S. Density functional theory based modeling of the corrosion on iron surfaces. *Arch. Metall. Mater.* **2013**, *58*, 321–323. [CrossRef]
16. Zheng, Y.-T.; Xuan, F.-Z.; Wang, Z. The Role of Atomic Structures on the Oxygen Corrosion of Polycrystalline Copper Surface. *Procedia Eng.* **2015**, *130*, 1184–1189. [CrossRef]
17. Liu, X.; Kim, S.-Y.; Lee, S.H.; Lee, B. Atomistic investigation on initiation of stress corrosion cracking of polycrystalline Ni60Cr30Fe10 alloys under high-temperature water by reactive molecular dynamics simulation. *Comput. Mater. Sci.* **2021**, *187*, 110087. [CrossRef]
18. Verners, O.; van Duin, A.C.T. Comparative molecular dynamics study of fcc-Ni nanoplate stress corrosion in water. *Surf. Sci.* **2015**, *633*, 94–101. [CrossRef]
19. DorMohammadi, H.; Pang, Q.; Arnadottir, L.; Isgor, O.B. Atomistic simulation of initial stages of iron corrosion in pure water using reactive molecular dynamics. *Comput. Mater. Sci.* **2018**, *145*, 126–133. [CrossRef]
20. DorMohammadi, H.; Pang, Q.; Murkute, P.; Árnadóttir, L.; Burkan Isgor, O. Investigation of iron passivity in highly alkaline media using reactive-force field molecular dynamics. *Corros. Sci.* **2019**, *157*, 31–40. [CrossRef]
21. DorMohammadi, H.; Pang, Q.; Murkute, P.; Árnadóttir, L.; Isgor, O.B. Investigation of chloride-induced depassivation of iron in alkaline media by reactive force field molecular dynamics. *Npj Mater. Degrad.* **2019**, *3*, 19. [CrossRef]
22. Lu, K.; Huo, C.-F.; He, Y.; Yin, J.; Liu, J.; Peng, Q.; Guo, W.-P.; Yang, Y.; Li, Y.-W.; Wen, X.-D. Grain boundary plays a key role in carbon diffusion in carbon irons revealed by a ReaxFF study. *J. Phys. Chem. C* **2018**, *122*, 23191–23199. [CrossRef]
23. Plimpton, S. Fast parallel algorithms for short-range molecular dynamics. *J. Comput. Phys.* **1995**, *117*, 1–19. [CrossRef]
24. Van Duin, A.C.; Dasgupta, S.; Lorant, F.; Goddard, W.A. ReaxFF: A reactive force field for hydrocarbons. *J. Phys. Chem. A* **2001**, *105*, 9396–9409. [CrossRef]
25. Huang, Y.; Hu, C.; Xiao, Z.; Gao, N.; Wang, Q.; Liu, Z.; Hu, W.; Deng, H. Atomic insight into iron corrosion exposed to supercritical water environment with an improved Fe-H_2O reactive force field. *Appl. Surf. Sci.* **2021**, *580*, 152300. [CrossRef]
26. Smith, D.W. A new method of estimating atomic charges by electronegativity equilibration. *J. Chem. Educ.* **1990**, *67*, 559. [CrossRef]
27. Rappe, A.K.; Goddard, W.A., III. Charge equilibration for molecular dynamics simulations. *J. Phys. Chem.* **1991**, *95*, 3358–3363. [CrossRef]
28. McDonald, I. NpT-ensemble Monte Carlo calculations for binary liquid mixtures. *Mol. Phys.* **1972**, *23*, 41–58. [CrossRef]
29. Hoover, W.G. Canonical dynamics: Equilibrium phase-space distributions. *Phys. Rev. A* **1985**, *31*, 1695. [CrossRef]
30. Nosé, S. A molecular dynamics method for simulations in the canonical ensemble. *Mol. Phys.* **1984**, *52*, 255–268. [CrossRef]
31. Assowe, O.; Politano, O.; Vignal, V.; Arnoux, P.; Diawara, B.; Verners, O.; Van Duin, A. Reactive molecular dynamics of the initial oxidation stages of Ni (111) in pure water: Effect of an applied electric field. *J. Phys. Chem. A* **2012**, *116*, 11796–11805. [CrossRef]
32. Das, N.K.; Suzuki, K.; Takeda, Y.; Ogawa, K.; Shoji, T. Quantum chemical molecular dynamics study of stress corrosion cracking behavior for fcc Fe and Fe–Cr surfaces. *Corros. Sci.* **2008**, *50*, 1701–1706. [CrossRef]
33. Wang, H.; Han, E.-H. Ab initio molecular dynamics simulation on interfacial reaction behavior of Fe-Cr-Ni stainless steel in high temperature water. *Comput. Mater. Sci.* **2018**, *149*, 143–152. [CrossRef]
34. Scott, R. *Computer Simulation of Liquids*; JSTOR: New York, NY, USA, 1991.
35. Frenkel, D.; Smit, B. *Understanding Molecular Simulation: From Algorithms to Applications*; Elsevier: Amsterdam, The Netherlands, 2001; Volume 1.